

HIGH-TEMPERATURE THERMODYNAMIC PROPERTIES
OF SOME LEAD-RHODIUM ALLOYS

By
Madhukar Mehta

ProQuest Number: 10795684

All rights reserved

INFORMATION TO ALL USERS

The quality of this reproduction is dependent upon the quality of the copy submitted.

In the unlikely event that the author did not send a complete manuscript and there are missing pages, these will be noted. Also, if material had to be removed, a note will indicate the deletion.



ProQuest 10795684

Published by ProQuest LLC (2018). Copyright of the Dissertation is held by the Author.

All rights reserved.

This work is protected against unauthorized copying under Title 17, United States Code
Microform Edition © ProQuest LLC.

ProQuest LLC.
789 East Eisenhower Parkway
P.O. Box 1346
Ann Arbor, MI 48106 – 1346

A Thesis submitted to the Faculty and the Board of Trustees of the Colorado School of Mines in partial fulfillment of the requirements for the degree of Master of Science.

Signed: Madhukar Mehta
Madhukar Mehta

Golden, Colorado

Date: Oct 29, 1968

Approved: John P. Hager
John P. Hager
Thesis Advisor

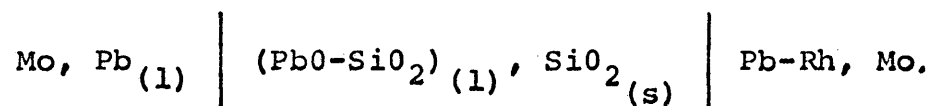
Paul G. Herold
Paul G. Herold
Head of Department
Metallurgical Engineering

Golden, Colorado

Date: Oct 29, 1968

ABSTRACT

The thermodynamic properties of the lead-rhodium system have been determined between 725°C and 1000°C by using the cell



The range of compositions studied was from $X_{\text{Pb}} = 0.61$ to $X_{\text{Pb}} = 0.90$. The activities of lead exhibit negative deviation from ideal behavior. A portion of the liquidus curve of the phase diagram was defined.

TABLE OF CONTENTS

	Page
INTRODUCTION	1
The Galvanic Cell Technique	1
Limitations of the Galvanic Cell.	3
Outline of This Study	4
LITERATURE SURVEY.	6
The Lead Oxide-Silica System.	6
The Lead-Rhodium System	8
APPARATUS AND EXPERIMENTAL PROCEDURE	9
Apparatus	9
Experimental Procedure.	13
Materials Preparation.	13
Operating Procedure.	13
REDUCTION OF EXPERIMENTAL DATA	15
Computation of Thermodynamic Values	15
Use of Computer	17
Estimation of Uncertainties	17
Uncertainty in the Temperature Readings.	18
Uncertainty in the Emf and $(\partial E/\partial T)$	18
Uncertainty in the Chemical Analysis	18
Uncertainty in the Activity of Lead.	19

	Page
Uncertainties in G_{Pb}^M , H_{Pb}^M , and S_{Pb}^M	19
Uncertainties in G_{Pb}^E and S_{Pb}^E	20
RESULTS.	21
ANALYSIS OF RESULTS.	33
Probable Sources of Errors.	33
The Phase Diagram	35
Comparison with Models of Metallic Solutions.	37
CONCLUSIONS.	39
SUGGESTIONS FOR FURTHER WORK	40
APPENDIX I	42
APPENDIX II.	43
APPENDIX III	44
BIBLIOGRAPHY	46

LIST OF FIGURES

Figure	Page
1. The lead-oxide-silica system	7
2. Galvanic cell design	10
3. Schematic view of the equipment.	12
4. Experimental data for the lead-rhodium system. .	22
5. Activity of lead for liquid Pb-Rh alloys at 900°C	25
6. Activity coefficients of lead for liquid Pb-Rh alloys at 900°C.	26
7. Partial molar free energies of mixing of lead in liquid Pb-Rh alloys at 900°C.	27
8. Partial molar entropies of mixing of lead in liquid Pb-Rh alloys at 900°C	28
9. Partial molar heats of mixing of lead in liquid Pb-Rh alloys at 900°C	29
10. Excess partial molar free energies of mixing of lead in liquid Pb-Rh alloys at 900°C .	31
11. Excess partial molar entropies of mixing of lead in liquid Pb-Rh alloys at 900°C.	32
12. Liquidus portion of the Pb-Rh system	36

LIST OF TABLES

Table	Page
1. Normal equations for liquid Pb-Rh alloys	23
2. Thermodynamic properties of lead in liquid Pb-Rh alloys at 900°C.	24
3. Excess partial molar properties, alpha and beta functions of lead in liquid Pb-Rh at 900°C.	30

ACKNOWLEDGMENTS

The author wishes to express his sincere appreciation to Dr. John Hager for his valuable guidance during this study.

Thanks are also expressed to Dr. Albert Schlechten and the Institute of Extractive Metallurgy for providing financial support to the author for the duration of this study. Thanks are also due to International Nickel Corporation for providing funds for the purchase of rhodium and other materials.

The author also wishes to thank Hewlett Packard for donating a differential voltmeter for this study.

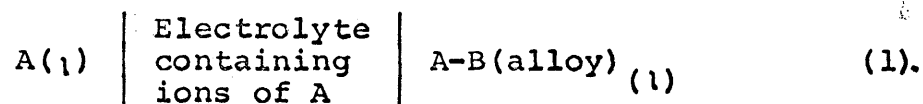
INTRODUCTION

The study of high temperature processes and of systems at high temperatures is of growing concern to the metallurgist, both for industrial applications and for basic research. The galvanic cell is a technique to evaluate thermodynamic data of systems at high temperatures.

The object of this study was to investigate the thermodynamic properties of the liquid lead-rhodium system through a portion of the compositional range by means of the galvanic cell technique using a molten oxide electrolyte.

The Galvanic Cell Technique

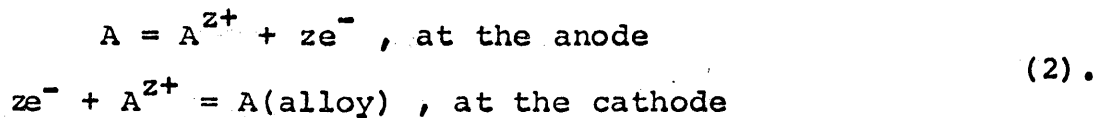
Consider a galvanic cell of the type



The electromotive force of this cell permits us to evaluate the thermodynamic properties of the alloy.

In the above cell, the more electropositive component A of the alloy is used as the anode; an alloy of A is used as the cathode; and an electrolyte containing ions of A is used to provide the bridge between the two electrodes.

The half reactions are



The overall reaction for the passage of Z faradays of positive electricity is



The free energy change in the cell is

$$\Delta G = -zFE \quad (4)$$

where,

ΔG = the Gibbs free energy change for reaction (3)

E = the emf of the cell in volts

z = the valence of A in the electrolyte

F = Faraday's number.

Equation (4) can be written as

$$\Delta G = \Delta G^{\circ} + RT \ln a_A = -zFE \quad (5)$$

If pure liquid A is chosen as the standard state of A in the alloy, then

$$\Delta G^{\circ} = 0.$$

Therefore, equation (5) becomes

$$\Delta G = RT \ln a_A = G_A^M = -zFE \quad (6)$$

where,

G_A^M = the partial molar free energy of mixing of A in the alloy

a_A = the Raoultian activity of A in the alloy.

The partial molar enthalpy can be determined from a knowledge of the change in emf with temperature:

$$S_A^M = -(\partial G_A^M / \partial T)_{X_A} = zF(\partial E / \partial T)_{X_A} \quad (7).$$

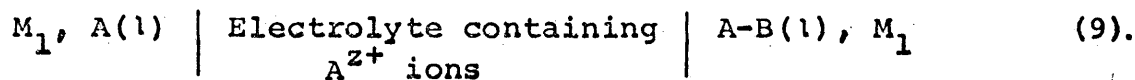
Similarly, the partial molar enthalpy can be calculated:

$$H_A^M = G_A^M + TS_A^M = -zF\{E - T(\partial E / \partial T)_{X_A}\} \quad (8).$$

Limitations of the Galvanic Cell

The use of a concentration cell between a pure metal and one of its alloys was first introduced by Taylor⁽¹⁾. The technique has been used extensively in determining basic thermodynamic functions and, more recently, in evaluating thermodynamic interactions in multi-component systems.

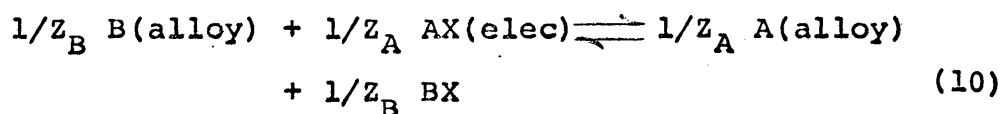
In a cell of the type



It is possible to have certain side reactions besides those shown in equation (2). Certain limitations have to be placed and some conditions met to reduce the errors in the final thermodynamic values. They are as follows:

1. The composition of the phases at each electrode are fixed and must remain unchanged by keeping the cell open-circuited. Hence, no side reactions should occur between the electrolyte and the lead wires, the crucible, or the cell atmosphere.

2. The electrolyte should possess only ionic conductivity because the presence of any electronic conductivity will result in a lower emf due to the transport of electrons through the electrolyte. The ionic conductance, therefore, should be maintained at a constant value $z+$.
3. The ions of A must be present in only one valence state. The valence state must be known to allow computation of thermodynamic properties.
4. Displacement reactions must be kept at a minimum. Wagner and Werner⁽²⁾ have shown that the displacement reaction



for the cell of the shown in equation (9), occurring at the alloy-electrolyte interface, should be extremely small. They have shown that the percentage of error in the activity of A due to the displacement reaction can be calculated by

$$\epsilon = (K/X_A) 100$$

where

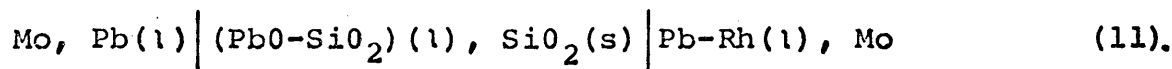
ϵ = the percentage of error in the activity of A

K = the equilibrium constant for reaction (10)

X_A = the mole fraction of A in the alloy.

Outline of This Study

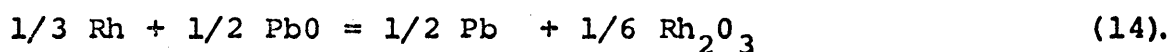
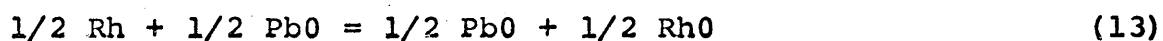
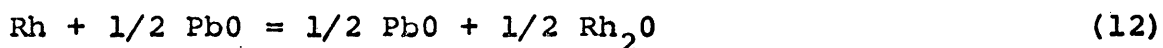
The galvanic cell used to measure the thermodynamic properties of the liquid lead-rhodium system was



All of the limitations mentioned in the last section are kept at a minimum by using this cell.

The reaction of the electrolyte with the silica crucible is prevented by keeping the electrolyte saturated with silica. The molybdenum lead wires do not react with the metal and alloy. The argon atmosphere in the cell prevents any reactions with the gas phase. Sealing the molybdenum wires inside silica tubes prevents any contact of the wire with the electrolyte.

In this case the displacement reactions will be:



It has been shown by Hager and Wilkomirsky⁽³⁾ and by Hager and Walker⁽⁴⁾ that the error in the activity of lead was negligible when the oxides involved were those of silver and gold, respectively. Since rhodium is as noble as silver and gold, it can be assumed that the error due to the displacement reaction is negligible.

LITERATURE SURVEY

A survey was made of the literature to find thermodynamic data for the PbO-SiO_2 and Pb-Rh systems.

The Lead Oxide - Silica System

The phase diagram has been investigated by Krakau and Vakhramer⁽⁵⁾ and by Geller, Creamer, and Bunting⁽⁶⁾. The diagram by Krakau and Vakhrameev is shown in Fig. 1.

Callow⁽⁷⁾ derived activities of PbO and SiO_2 in the system $\text{PbO} + \text{SiO}_2$ from data on rates of volatilization determined by Preston and Turner⁽⁸⁾. Activities of PbO in SiO_2 melts have also been determined by Richardson and Webb⁽⁹⁾, and Ito and Yanagese⁽¹⁰⁾.

Shartis and Newman⁽¹¹⁾ have determined the heats of formation of PbO-SiO_2 mixtures at room temperature. The free energy of formation of PbO in PbO-SiO_2 has been investigated by Sridhar and Jeffre⁽¹²⁾, who used emf measurements on high temperature galvanic cells.

Bockris, Kitchener, and Davis⁽¹³⁾, and Bockris and Mellors⁽¹⁴⁾ have shown that PbO-SiO_2 melts exhibit only ionic conductance. The same conclusion was reached more recently by Hager and Wilkomirsky⁽³⁾, and by Hager and Walker⁽⁴⁾.

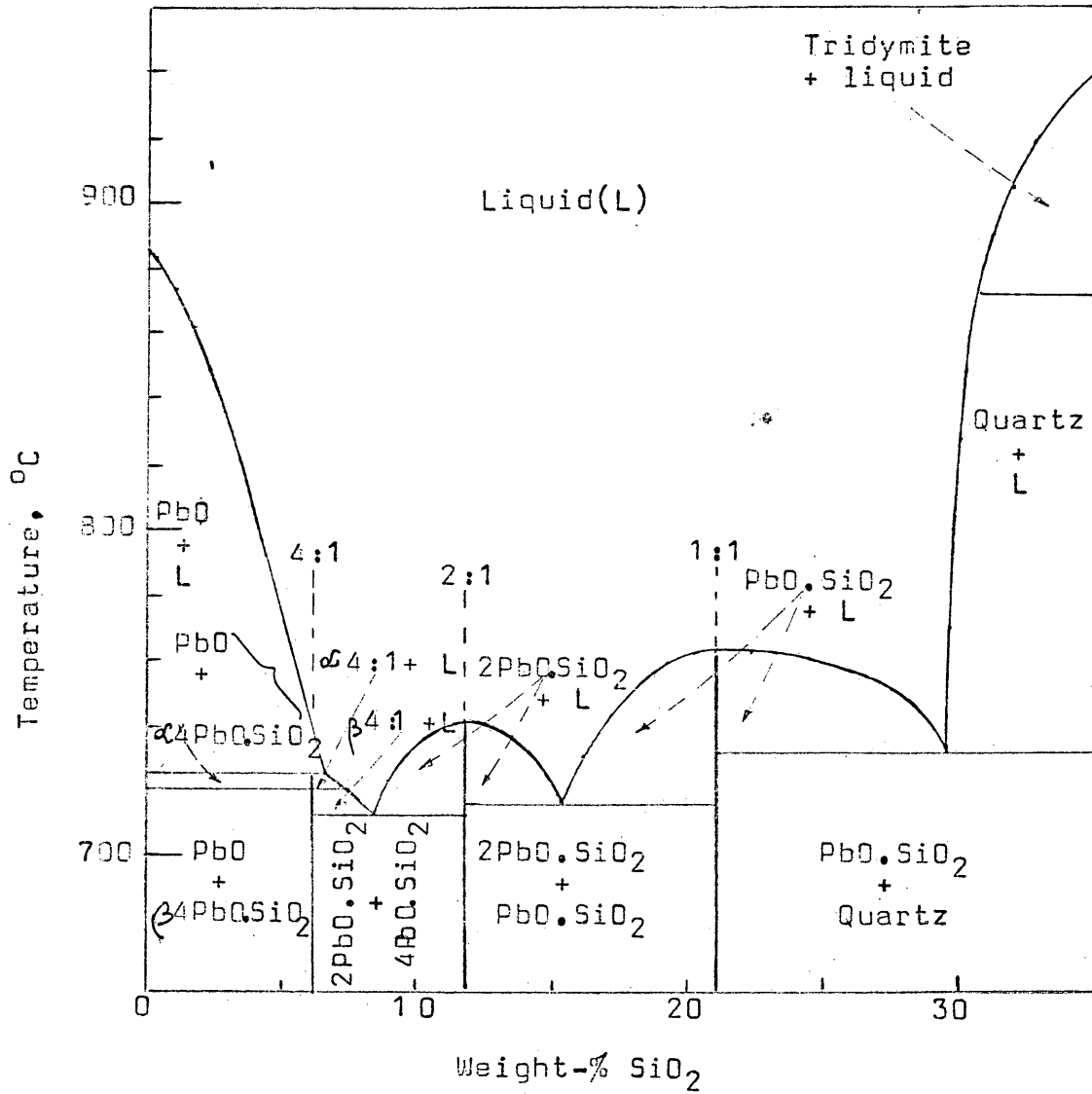


Fig. 1. The lead oxide-silica equilibrium diagram.

The Lead-Rhodium System

In the literature there is no data on the phase diagram or the thermodynamic properties of the lead-rhodium system.

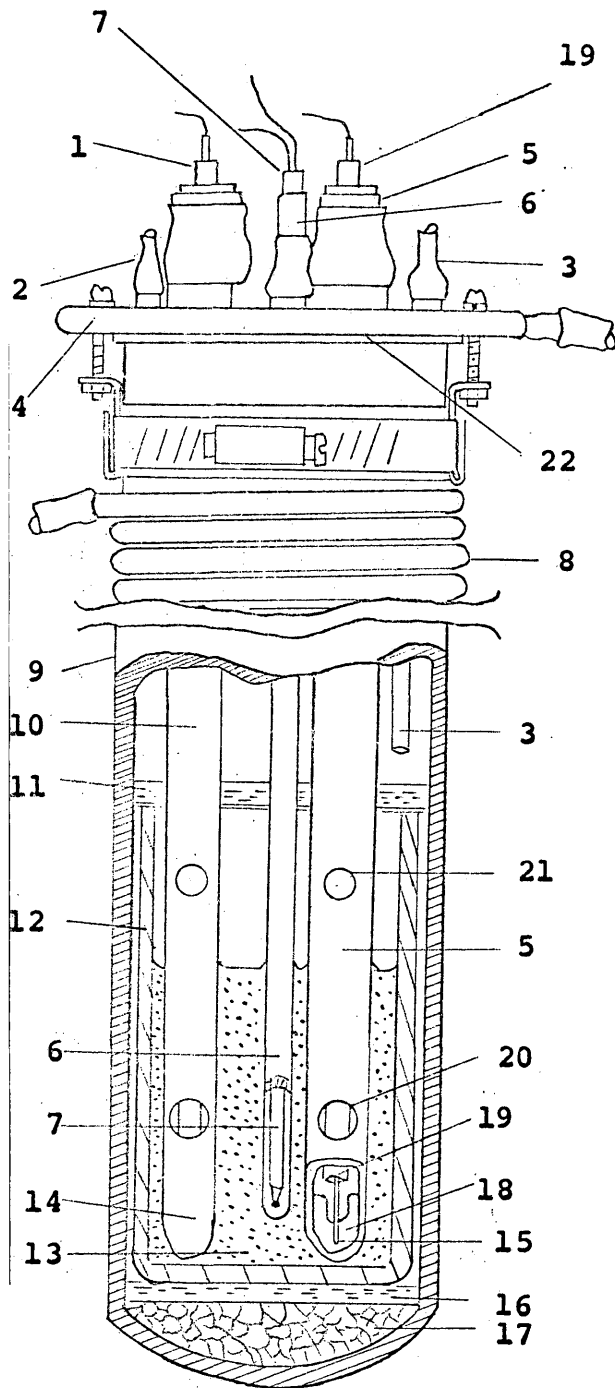
APPARATUS AND EXPERIMENTAL PROCEDURE

The experimental procedure consisted mainly in the use of a reversible galvanic cell to determine the chemical potential of lead in homogeneous liquid lead-rhodium alloys in the compositional range 0.90 to 0.61 mole percent of lead for the temperature interval 700°C to 950°C. A relationship between emf and temperature was determined for each of the alloys studied.

Apparatus

The galvanic cell arrangement is shown in Fig. 2. The electrolyte was contained in a crucible made of pure opaque quartz with the dimensions 1-3/8 in. ID by 4 in. high. The entire cell was contained in a mullite tube, 2 in. ID. The alloy electrode container was a 10-mm-ID transparent quartz tube. The standard electrode was contained in a 7-mm-ID transparent quartz tube. Each one of the electrode tubes had two holes blown near the closed end, the lower hole for completing the electrolyte bridge and the upper for gas release. The electrode leads were 0.05-in.-diam molybdenum wires protected by 2-mm-ID quartz tubing.

The temperature inside the cell was measured by a Pt,



1. Alloy Electrode Lead Wire in Quartz Tube
2. Argon Inlet
3. Argon Outlet
4. Water-Cooled Brass Head
5. Standard Electrode Quartz Tubing
6. Quartz Thermocouple Protection Tube
7. Pt, Pt-Rh Measuring Thermocouple
8. Copper Cooling Coil
9. Mullite Reaction Tube
10. Alloy Electrode Quartz Tubing
11. Alumina Crucible Cover
12. Quartz Crucible
13. PbO-SiO₂ Electrolyte
14. Pb-Rh Alloy Electrode
15. Molybdenum Electrode Lead Wire
16. Alumina Crucible Support
17. Porcelain Beads
18. Pb Standard Electrode
19. Standard Electrode Lead Wire in Quartz Tubing
20. Electrolyte Window
21. Gas Vent
22. Silicon Rubber Gasket

Figure 2. Galvanic cell design.

Pt-10%Rh thermocouple calibrated against the melting point of pure silver (960.8°C) and the Ag-Cu eutectic (779.8°C)⁽¹⁵⁾. The calibration of the thermocouple is shown in Appendix II. The thermocouple was insulated by high purity alumina and housed in a 3-mm-ID quartz tubing. The protective tubing of the thermocouple was submerged in the electrolyte.

A water-cooled brass head with suitable fittings permitted the entry of the standard electrode tube, the alloy tube, and the thermocouple protection tube. The reaction tube was connected to a three-way valve to permit either application of a vacuum or argon gas to the cell. Two bubblers containing dibutyl phthalate provided a gas seal for the reaction tube.

The reaction tube was inserted in a vertical Marshall resistance furnace. Temperature control was by means of a Foxboro electro-mechanical controller, with the controlling thermocouple inserted between the furnace and the reaction tube. The temperature was kept within $\pm 1^{\circ}\text{C}$. A schematic view of the equipment arrangement is shown in Fig. 3.

Potentials of the cell and the thermocouple were measured with a Leeds and Northrup potentiometer Model 7552 and a differential voltmeter. The limits of error in the readings were 0.04 percent of reading + $3\mu\text{V}$.

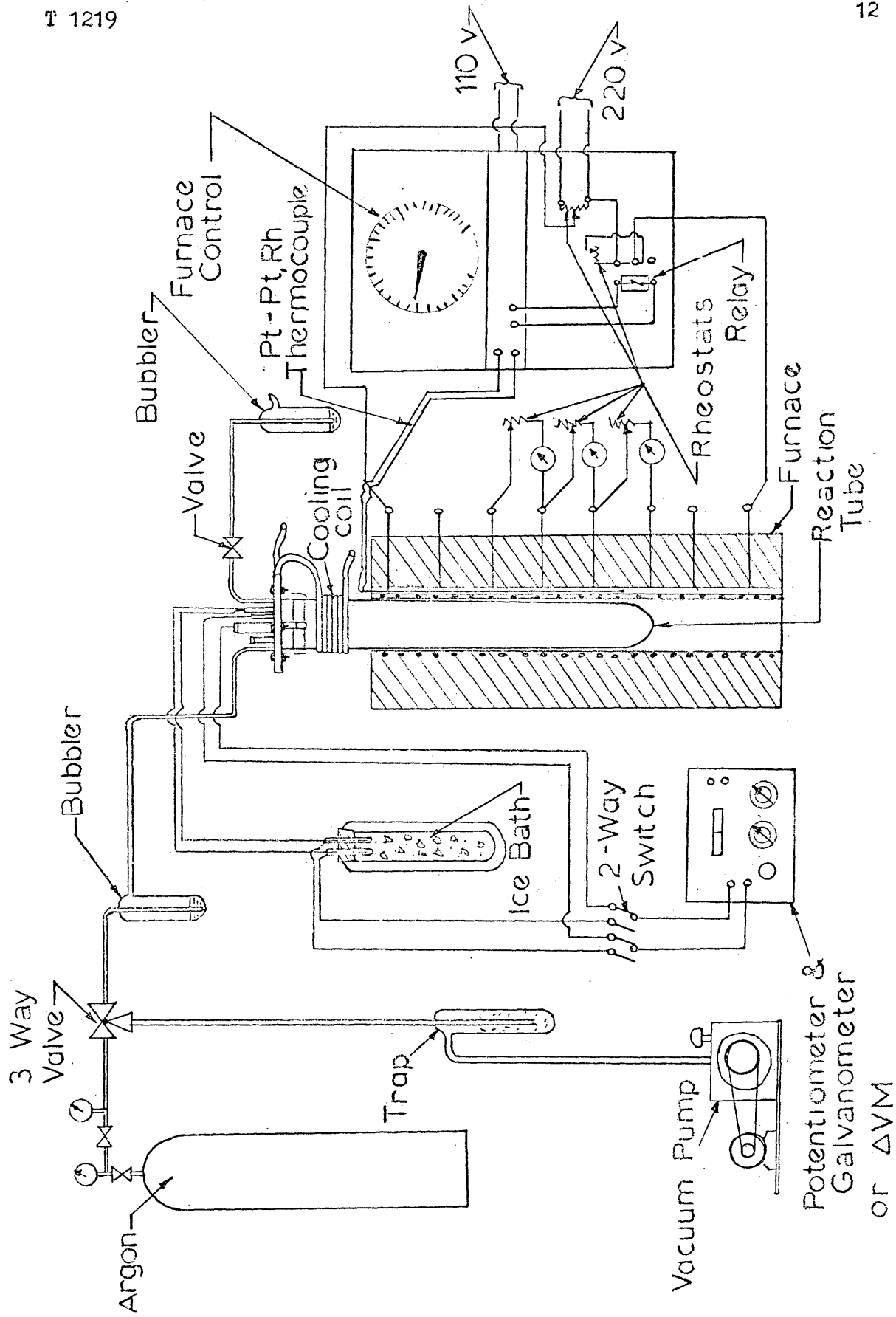


Figure 3: Schematic view of the equipment.

Experimental Procedure

The experimental procedure involved (1) materials preparation and (2) operating procedure.

Materials Preparations. The initial step in assembling the cell was the preparation of the electrolyte. The electrolyte was prepared in batches of 2700 g by melting a mixture of 67 wt-% PbO and 33 wt-% SiO₂. The lead oxide was 99.9 percent pure, and the silica was of pure chromatographic grade, 50/200 mesh. The PbO-SiO₂ mixture was heated in a 525 cc silica crucible in a gas-fired muffle furnace at 1000°C for three hours. The melt was cast in a steel mold and then crushed to -6 mesh. During this study three different batches of electrolyte were prepared with no detectable difference in cell performance. All of the electrolyte exhibited the same pale yellow color with some precipitated silica.

The alloys were prepared with high purity lead and rhodium which assayed 99.99+ percent purity. The lead was in granular form, but the rhodium was cut in small pieces from a 0.020-in.-diam wire.

Operating Procedure. After adding about 200 grams of the electrolyte to the cell crucible, the cell was assembled as shown in Fig. 2. After the reaction tube was evacuated, a slow flow of argon was started while the furnace was heated slowly to about 950°C. At this temperature both the

standard electrode and the alloy electrode were lowered into the cell. The cell was held at 950°C for 24 hours to allow the alloy and the electrolyte to reach equilibrium. The emf readings were then taken, approximately, in the following manner: 950-900-850-800-750-775-825-925°C, allowing about four hours for the cell to reach equilibrium after each change in temperature. At the end of this period, readings were taken every 15 minutes until a constant value was obtained. After the complete temperature range was studied, the alloy tube was removed, and a new alloy tube was lowered into the crucible. Again 24 hours were allowed for the new alloy to homogenize.

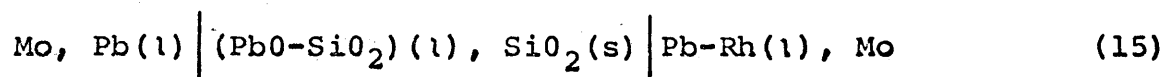
The potentiometer was used in reading the emf and the temperature above 800°C. Below this temperature when the electrolyte was viscous the differential voltmeter was used. The power to the furnace had to be shut off when the emf was being read in order to reduce any induced emf.

REDUCTION OF EXPERIMENTAL DATA

The raw experimental data was reduced to meaningful thermodynamic values by the equations listed in this section. The computer was used to fit the best straight line through the data points for the E vs T plots using the method of least squares. An analysis of the uncertainties of each thermodynamic property is also presented in this section to show the limits of accuracy.

Computation of Thermodynamic Values

The galvanic cell of the type



has the following nominal cell reaction:



The change in free energy for this reaction is given by

$$\Delta G = \mu_{\text{Pb(alloy)}} - \mu_{\text{Pb(l)}}^{\circ} = G_A^M = RT \ln a_{\text{Pb}} = -zFE \quad (17)$$

where,

$\mu_{\text{Pb(alloy)}}$ = the chemical potential of the lead in the liquid alloy at temperature T

$\mu_{\text{Pb(l)}}^{\circ}$ = the chemical potential of pure liquid lead at T°C

F = Faraday's constant (23,063 cal/volt-equivalent)

E = the potential of the cell in volts

z = the number of equivalents of lead oxidized
at the anode

a_{Pb} = the activity of lead in the liquid alloy.

Rearranging equation (17), the activity of lead in the alloy can be calculated as follows:

$$a_{Pb(l)} = \exp(-zFE/RT) \quad (18).$$

The activity coefficient of lead, γ_{Pb} , is defined by

$$\gamma_{Pb} = a_{Pb}/X_{Pb} \quad (19).$$

The partial molar entropy of mixing of lead at constant pressure and composition is calculated from the slope of the E vs T plot as follows:

$$S_{Pb}^M = zF(\partial E/\partial T)_{P, X_{Pb}} \quad (20).$$

Similarly, the partial molar heat of mixing of lead is determined by:

$$\begin{aligned} H_{Pb}^M &= G_{Pb}^M + TS_{Pb}^M = -zFE + zFT(\partial E/\partial T)_{P, X_{Pb}} \\ &= -zF\{E - T(\partial E/\partial T)_{P, X_{Pb}}\} \end{aligned} \quad (21).$$

The excess partial molar properties of lead are defined by

$$G_{Pb}^E = G_{Pb}^M - G_{Pb}^M(\text{ideal}) = -zFE - RT \ln X_{Pb} = RT \ln \gamma_{Pb} \quad (22)$$

$$S_{Pb}^E = S_{Pb}^M - S_{Pb(ideal)}^M = zF(\partial E/\partial T)_{P, X_{Pb}} + RT \ln X_{Pb} \quad (23),$$

and the excess partial molar heat of mixing of lead is expressed by

$$H_{Pb}^E = H_{Pb}^M = G_{Pb}^E + TS_{Pb}^E \quad (24).$$

Use of the Computer

A computer program developed by Zambrano⁽¹⁶⁾ was used to calculate the thermodynamic properties from the experimental data. The least squares fit was used to fit lines through the experimental points. From the emf vs T equations obtained from this program, the thermodynamic values for lead were calculated by use of the computer.

Estimation of Uncertainties

If a quantity Q is a function of several independent measured quantities x, y, z, . . . , the error in Q due to errors $\delta x'$, $\delta y'$, $\delta z'$, . . . , is given by the equation⁽¹⁷⁾

$$\delta Q = (\partial Q/\partial x) \delta x' + (\partial Q/\partial y) \delta y' + (\partial Q/\partial z) \delta z' + \dots \quad (25).$$

The most probable value of Q is given by

$$\delta Q = \{ (\partial Q/\partial x)^2 (\delta x)^2 + (\partial Q/\partial y)^2 (\delta y)^2 + (\partial Q/\partial z)^2 (\delta z)^2 + \dots \}^{1/2} \quad (26)$$

where δx , δy , and δz are the maximum values of the errors $\delta x'$, $\delta y'$, and $\delta z'$.

Uncertainty in the Temperature Readings: The total uncertainty in the temperature is calculated from

a) Uncertainty in thermocouple calibration: $\pm 0.4^{\circ}\text{C}$,

(Appendix II)

b) Uncertainty due to drifts in temperature during the run, determined experimentally to be $\pm 0.5^{\circ}\text{C}$

When equation (26) is used the total uncertainty in temperature is

$$\delta T = \pm 0.6^{\circ}\text{C}$$

Uncertainty in the emf and $(\partial E/\partial T)$: The total uncertainty in E as determined by a least squares analysis was

$$\delta E < 0.5 \text{ v at } X_{\text{Pb}} = 0.73$$

The total uncertainty in $\partial E/\partial T$, also determined by a least squares analysis, was

$$\delta(\partial E/\partial T) = \pm 0.0004\text{mv}/^{\circ}\text{C}$$

Uncertainty in the Chemical Analysis: The mole fraction of lead was determined from the weights of lead and rhodium used in preparing the alloys. Since Zambrano⁽¹⁶⁾ found that the mole fraction of lead for the Pb-Ag-Au system calculated from the weights of the metals used was within the limits of error in the mole fraction of lead obtained by chemical analysis on the atomic absorption unit, no chemical analysis was performed in this study. However, the uncertainties in X_{Pb} obtained from chemical analysis on the atomic absorption

unit are used in this study and are presented below.

a) The maximum uncertainty in the chemical analyses of the standards was

$$\delta'X_{Pb} = \pm 0.0015.$$

b) The maximum uncertainty in the chemical analyses on the alloys was

$$\delta''X_{Pb} = \pm 0.008.$$

The total uncertainty in the mole fraction of lead was

$$\delta X_{Pb} = \{(\delta'X_{Pb})^2 + (\delta''X_{Pb})^2\}^{1/2} = \pm 0.008.$$

Uncertainty in the Activity of Lead: By combining equations (18) and (26) and solving for a_{Pb} , the uncertainty is

$$\delta a_{Pb} = \{[\exp(-zFE/RT) (zF/RT)]^2 [(\delta E)^2 + (E/T)^2 (\delta T)^2]\}^{1/2} \quad (27).$$

The error was calculated to be

$$\delta a_{Pb} = \pm 0.08 \text{ at } X_{Pb} = 0.73.$$

Uncertainties in G_{Pb}^M , H_{Pb}^M , and S_{Pb}^M : When equations (17), (20), and (21) are used in conjunction with equation (26), the following equations are obtained:

$$\delta G_{Pb}^M = \{(zF)^2 (\delta E)^2\}^{1/2} \quad (28)$$

$$\delta H_{Pb}^M = \{(zF\delta E)^2 + [zF(\partial E/\partial T)\delta T]^2 + [zFT\delta(\partial E/\partial T)]^2\}^{1/2} \quad (29)$$

$$\delta S_{Pb}^M = \{[zF\delta(\partial E/\partial T)]^2\}^{1/2} \quad (30).$$

From these equations, the following errors were obtained:

$$\delta G_{Pb}^M = \pm 23 \text{ cal}$$

$$\delta H_{Pb}^M = \pm 31 \text{ cal at } X_{Pb} = 0.9$$

$$\delta S_{Pb}^M = \pm 0.02 \text{ cal/deg.}$$

Uncertainties in G_{Pb}^E and S_{Pb}^E : From equations (22), (23),

and (26) the following equations are obtained:

$$\delta G_{Pb}^E = \{ (zF\delta E)^2 + R^2 [(\ln X_{Pb} \delta T)^2 + (T\delta X_{Pb}/X_{Pb})^2] \}^{1/2} \quad (31)$$

$$\delta S_{Pb}^E = \{ [zF\delta(\partial E/\partial T)]^2 + [R(\delta X_{Pb}/X_{Pb})]^2 \}^{1/2} \quad (32).$$

The errors calculated from the above equations were

$$\delta G_{Pb}^E = \pm 37 \text{ cal at } X_{Pb} = 0.65$$

$$\delta S_{Pb}^E = \pm 0.03 \text{ cal/deg at } X_{Pb} = 0.65.$$

RESULTS

The experimental data are presented in tabular form in Appendix I and graphically in Fig. 4. Normal equations for the cell potentials as a function of temperature have been calculated for the linear portions of the E vs T plots and tabulated in Table 1.

The data from Table 1 are combined with equations (17), (18), (19), (20), and (21) to give the thermodynamic properties of mixing of lead in liquid Pb-Rh alloys. The results are given in Table 2. The activities, activity coefficients, and the partial molar properties of mixing are plotted in Figs. 5, 6, 7, 8 and 9.

The excess partial molar free energy and entropy were calculated from equations (22) and (23). These values are shown in Table 3 along with the alpha and beta functions of lead. The excess partial molar functions are plotted in Figs. 10 and 11.

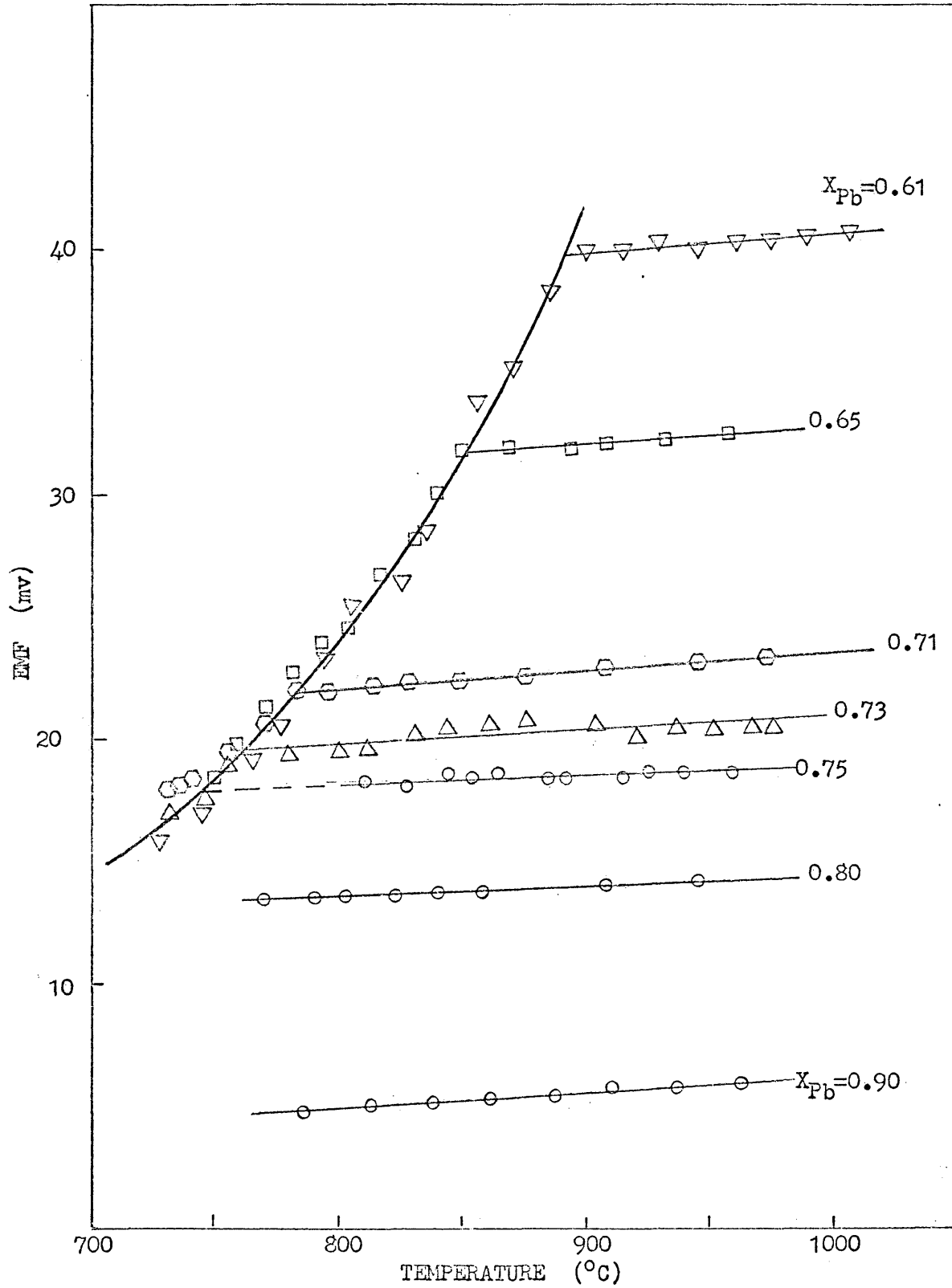


Figure 4: Experimental data for the lead-rhodium system.

Table 1. Normal equations for some liquid Pb-Rh alloys.

<u>X_{Pb}</u>	<u>E, mv (T=°C)</u>	<u>Temp. Range (T° C)</u>
0.90	$0.244 + 5.86 \times 10^{-3}T$	787 - 962
0.80	$10.51 + 3.89 \times 10^{-3}T$	770 - 946
0.75	$16.03 + 2.75 \times 10^{-3}T$	811 - 958
0.73	$15.25 + 5.62 \times 10^{-3}T$	781 - 980
0.71	$15.82 + 7.83 \times 10^{-3}T$	787 - 968
0.65	$26.01 + 6.75 \times 10^{-3}T$	849 - 956
0.61	$34.17 + 6.43 \times 10^{-3}T$	900 - 988

Table 2. Thermodynamic properties of lead in liquid lead-rhodium alloys at 900°C.

$\underline{X_{Pb}}$	$\underline{G_{Pb}^M}$	$\underline{a_{Pb}}$	$\underline{\gamma_{Pb}}$	$\underline{S_{Pb}^M}$	$\underline{H_{Pb}^M}$
0.90	- 254.6	0.896	0.996	0.270	62.6
0.80	- 646.7	0.758	0.947	0.180	-435.8
0.75	- 853.7	0.693	0.924	0.127	-704.7
0.73	- 936.7	0.669	0.917	0.259	-632.7
0.71	-1054.9	0.636	0.896	0.361	-631.0
0.65	-1479.8	0.530	0.815	0.311	-1114.5
0.61	-1843.0	0.454	0.748	0.297	-1495.0

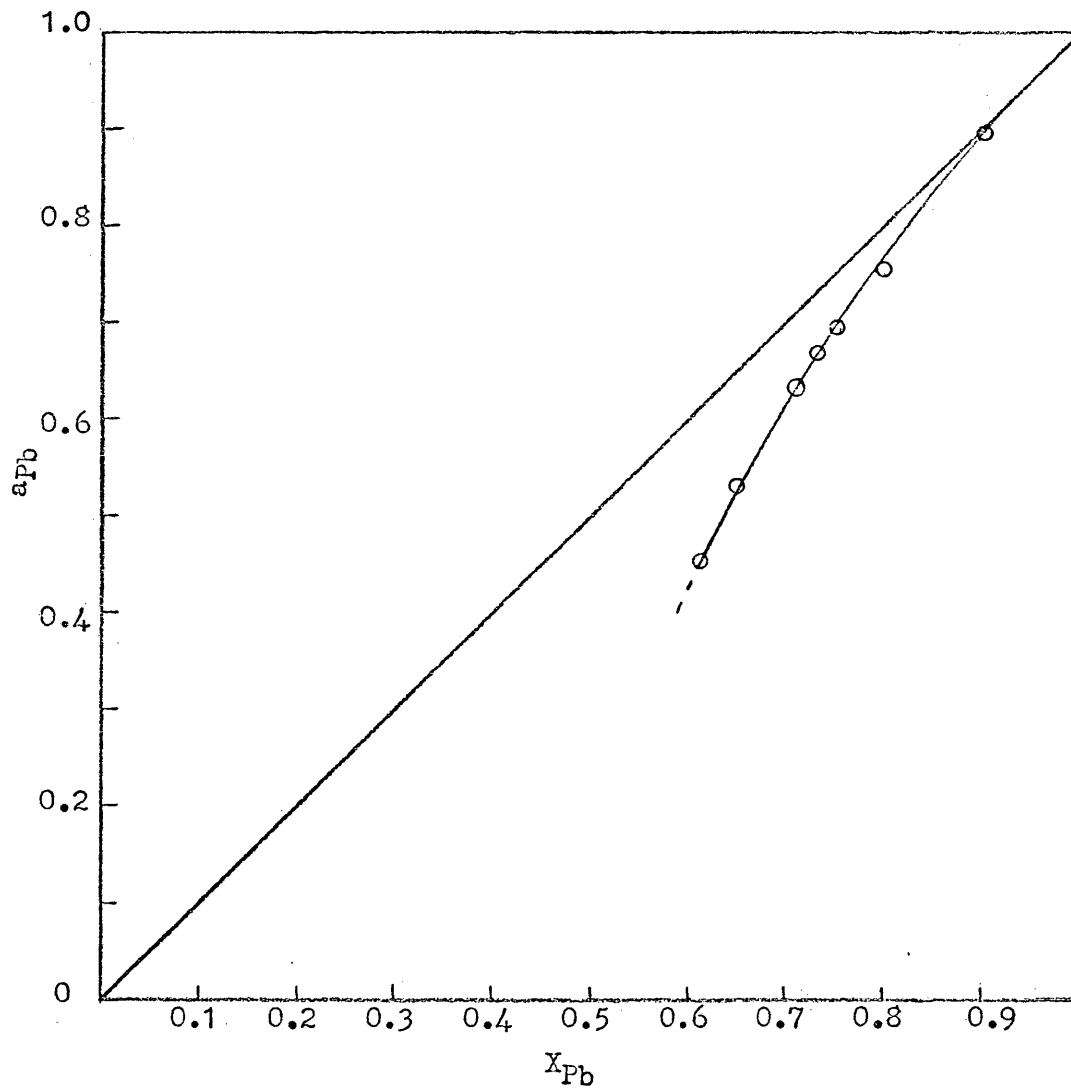


Figure 5: Activity of lead for liquid Pb-Rh at 900°C.

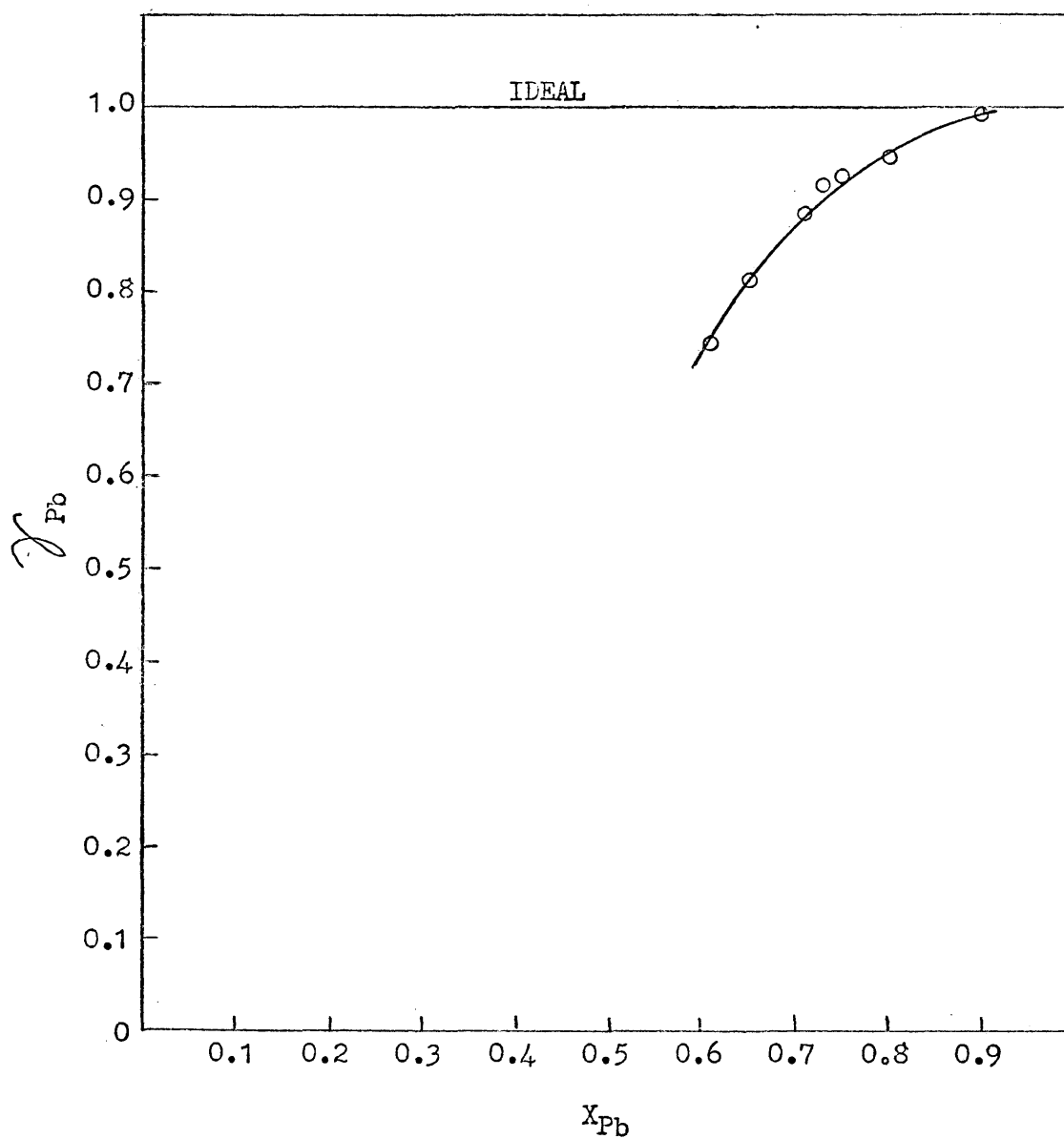


Figure 6: Activity coefficients of lead for liquid Pb-Rh at 900°C.

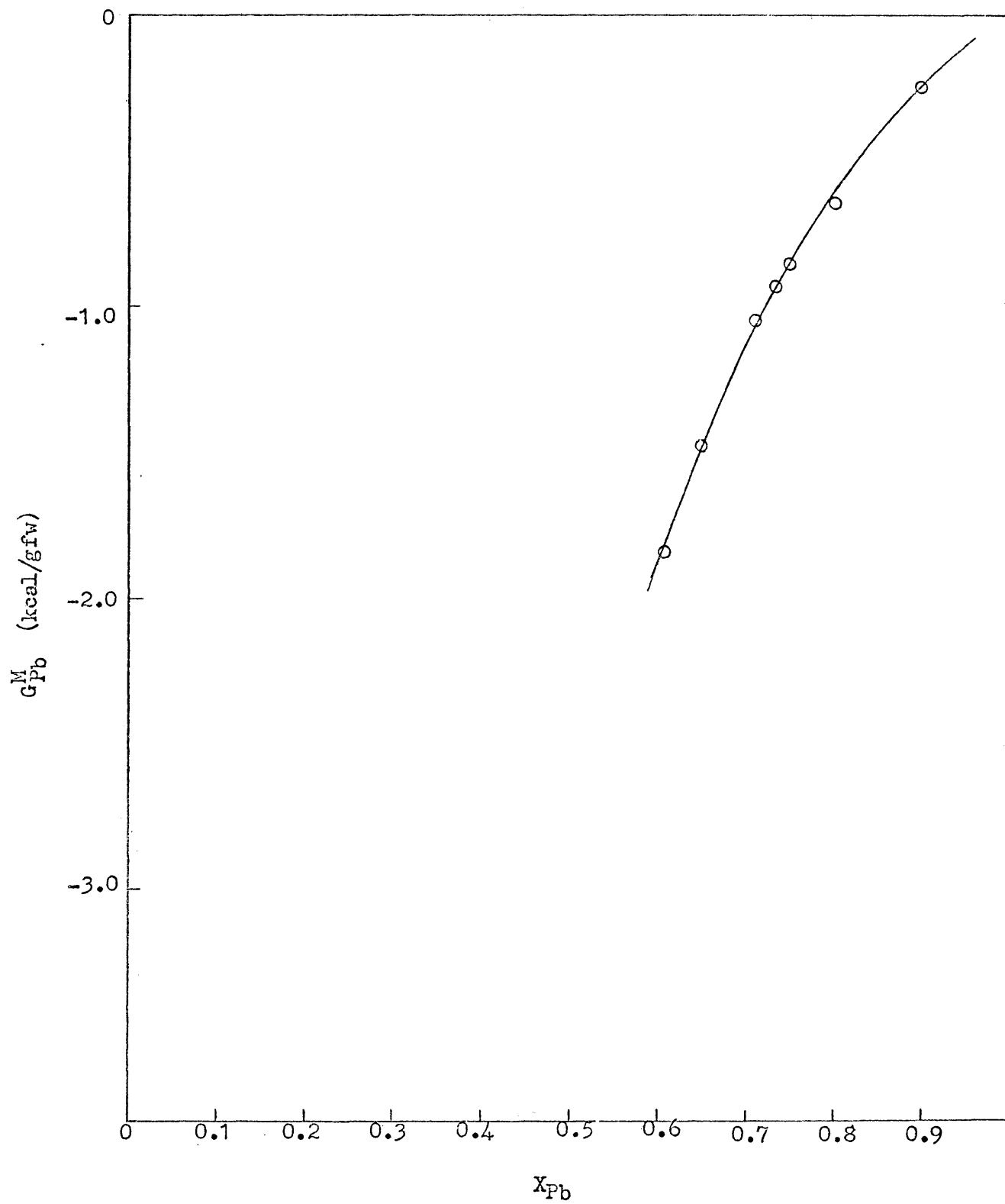


Figure 7: Partial molar free energy of mixing of lead in liquid Pb-Rh at 900°C.

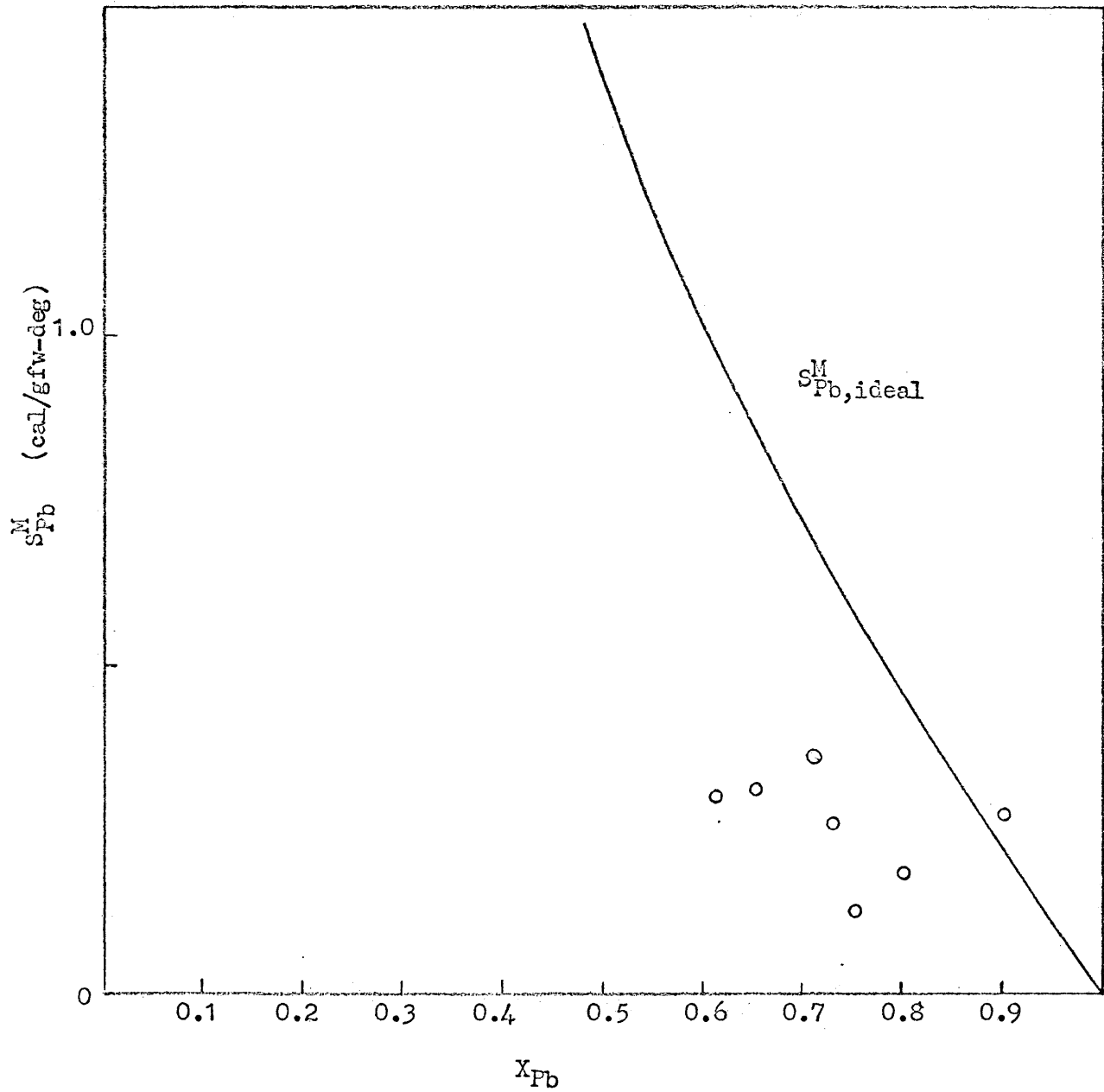


Figure 8: Partial molar entropy of mixing of lead in liquid Pb-Rh at 900°C.

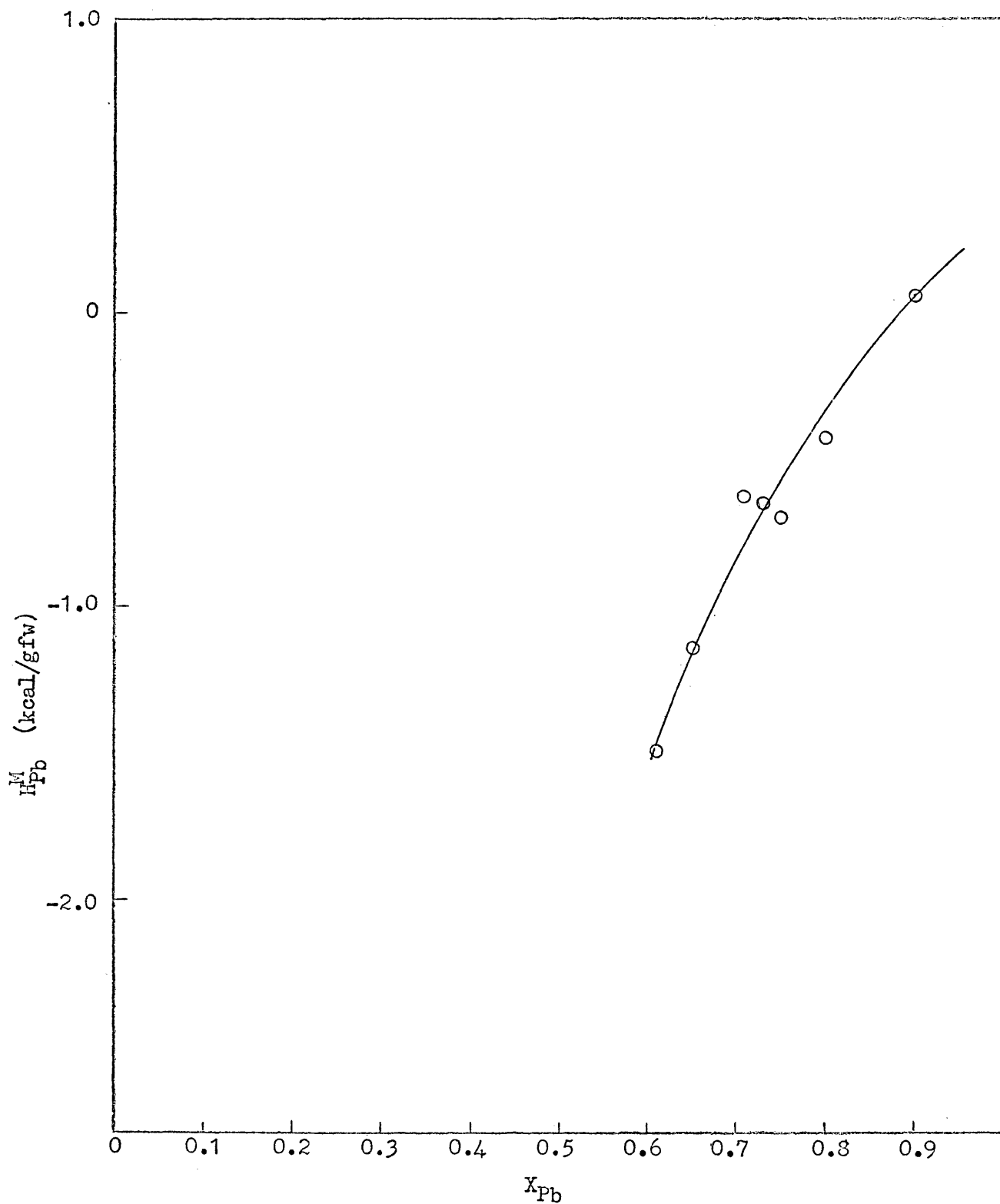


Figure 9: Partial molar heat of mixing of lead in liquid Pb-Rh at 900°C.

Table 3. Excess partial molar properties, alpha and beta functions of lead in liquid lead-rhodium at 900°C.

$\underline{x_{Pb}}$	$\underline{G_{Pb}^E}$	$\underline{S_{Pb}^E}$	$\underline{\alpha_{Pb}}$	$\underline{\beta_{Pb}}$
0.90	- 9.0	0.061	- 897	- 6257
0.80	-126.4	-0.267	-3161	-10896
0.75	-183.0	-0.445	-2928	-11274
0.73	-203.1	-0.366	-2785	- 8679
0.71	-256.45	-0.319	-3049	- 7503
0.65	-475.5	-0.545	-3882	- 9098
0.61	-690.7	-0.686	-4541	- 9829

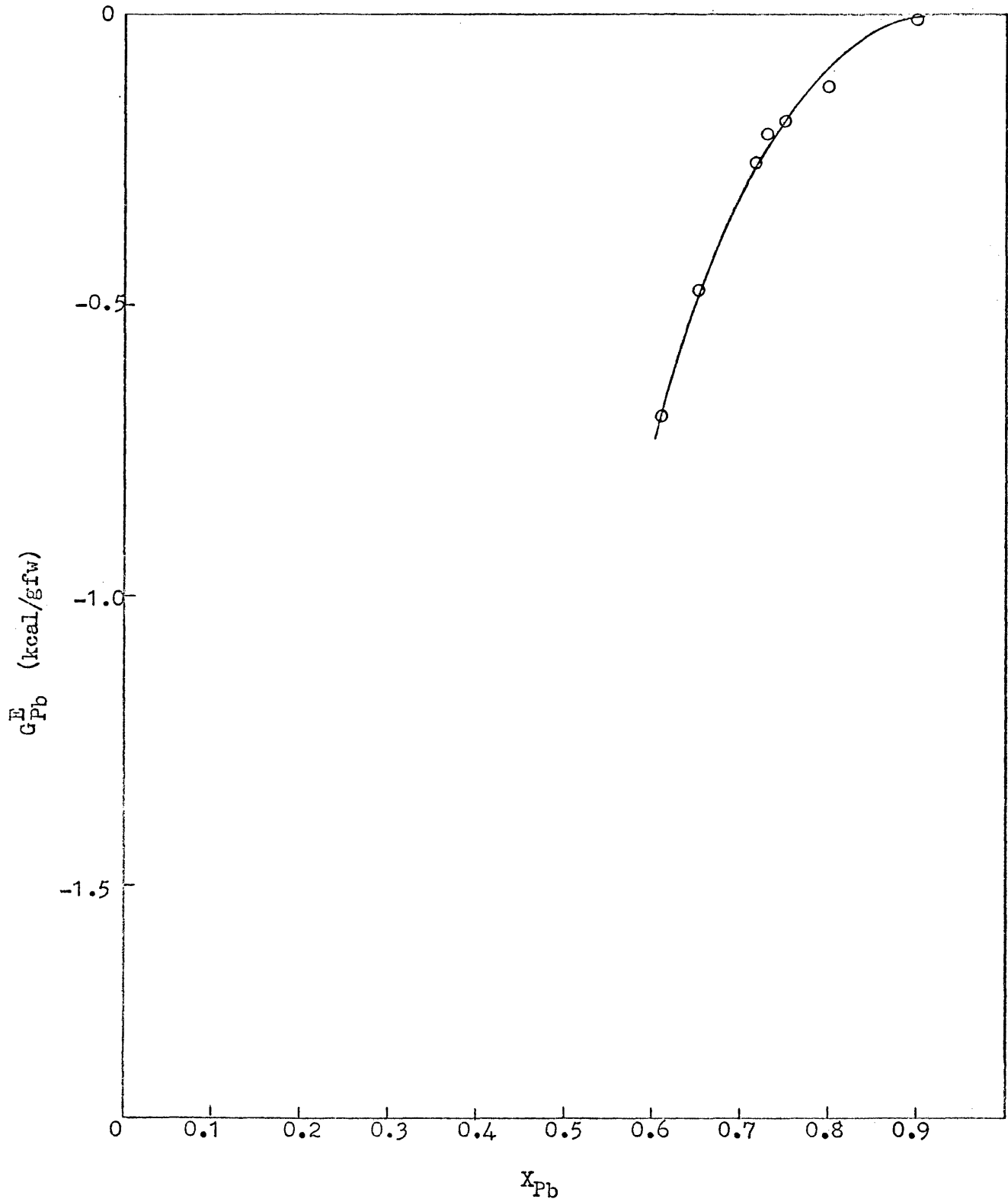


Figure 10: Excess partial molar free energy of mixing of lead in liquid Pb-Rh at 900°C.

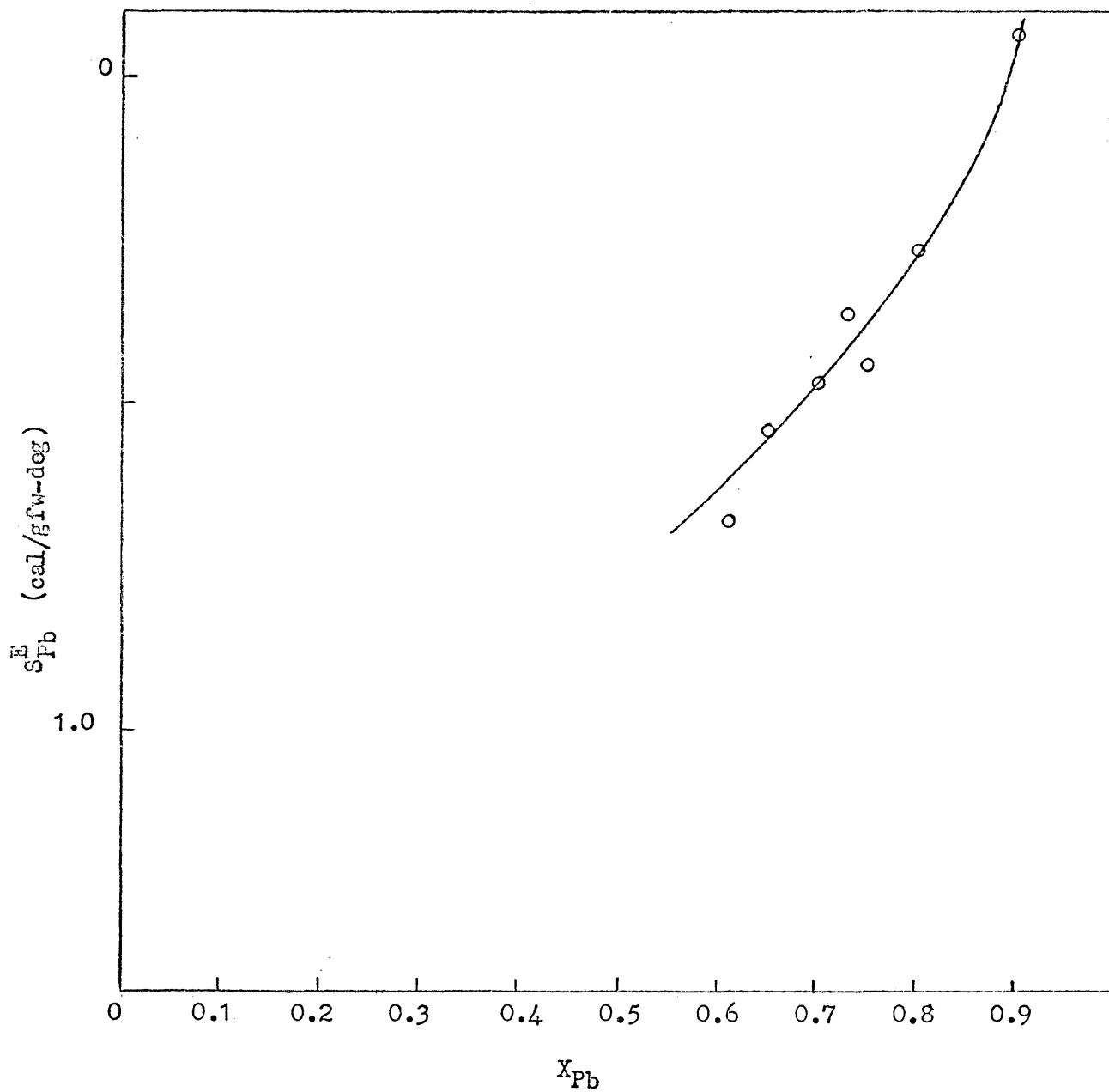


Figure 11: Excess partial molar entropy of mixing of lead in liquid Pb-Rh at 900°C.

ANALYSIS OF RESULTS

The preceding section listed the thermodynamic properties of lead in some liquid lead-rhodium alloys. In this section these results will be analyzed in terms of probable sources of errors, prediction of part of the phase diagram, and, finally, comparison of this study with models of metallic solutions.

Probable Sources of Errors

The three variables in this study were temperature, alloy composition, and emf. The emf is dependent on both the temperature and the alloy composition. The uncertainties in these three measured quantities were listed earlier.

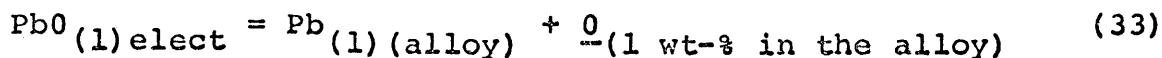
The cell potential was stable when the readings were taken. The emf was easily read between 800°C and 1000°C. However, below 800°C the electrolyte was very viscous, and a differential voltmeter (made by Hewlett Packard) had to be used. Hence, by the use of a potentiometer and a differential voltmeter, the emf could be read between 725°C and 1000°C. Above about 1000°C it was difficult to obtain constant readings. There is a possibility of concentration gradients in the electrolyte because silica saturation cannot be assured above 1000°C.

The electrolyte was always clear when removed after a series of runs. The crucible and electrode tubes showed no attack by the electrolyte; hence, the electrolyte was always saturated with silica. Further evidence of silica saturation was shown by small amounts of precipitated silica on the walls of the crucible. No electro-transport measurements were made, but it was assumed, from studies done by previous workers^{(3), (4)}, that electronic conductivity and tetravalent lead ions were absent.

The above factors show that the cell design and experimental technique were very adequate. Thus, if there is any lack of accuracy, it could be due only to either a displacement reaction or a dissociation reaction.

The displacement reactions were shown in equations (12), (13), and (14). No thermodynamic data exist for any of the oxides of rhodium. It is felt that the error involved in estimating the free-energy does not warrant a rigorous analysis of the error due to the displacement reaction. With the help of other studies made on silver⁽³⁾, gold⁽⁴⁾, and platinum^{(18), (19)}, it can be assumed that in the case of rhodium (which is as noble as silver, gold, and platinum) the error due to the displacement reaction is negligible.

Another error can arise from the dissociation reaction:



The above reaction can have two effects: the enrichment of lead in the alloy at the alloy-electrolyte interface, and the addition of oxygen to the lead-rhodium alloy.

The error resulting from the deposition of lead at the alloy-electrolyte interface may be presumed to be negligible since the drift in cell potential after alloy electrolyte equilibration was itself negligible.

Hager and Wilkomirsky⁽³⁾ have obtained the equilibrium wt-% oxygen for reaction (33) at 1000°C when $a_{Pb} = 1.0$, with the standard state for dissolved oxygen taken as 1 wt-% in lead. They have also estimated the equilibrium wt-% oxygen for the same reaction to be 4.8×10^{-5} for $a_{Pb} = 0.05$ at 1000°C when 1 wt-% oxygen in silver is taken as the standard state. If it is assumed that the wt-% oxygen dissolved in the high rhodium alloys is of about the same magnitude as that for silver, due to the nobility of rhodium, the effect of oxygen contamination for the alloys appears to be negligible.

The Phase Diagram

The phase diagram for the lead-rhodium system has not been determined. Some points determined from the liquidus line in Fig. 4 are plotted in Fig. 12. The range of composition of points plotted in Fig. 12 is from $X_{Pb} = 0.61$ to $X_{Pb} = 0.75$.

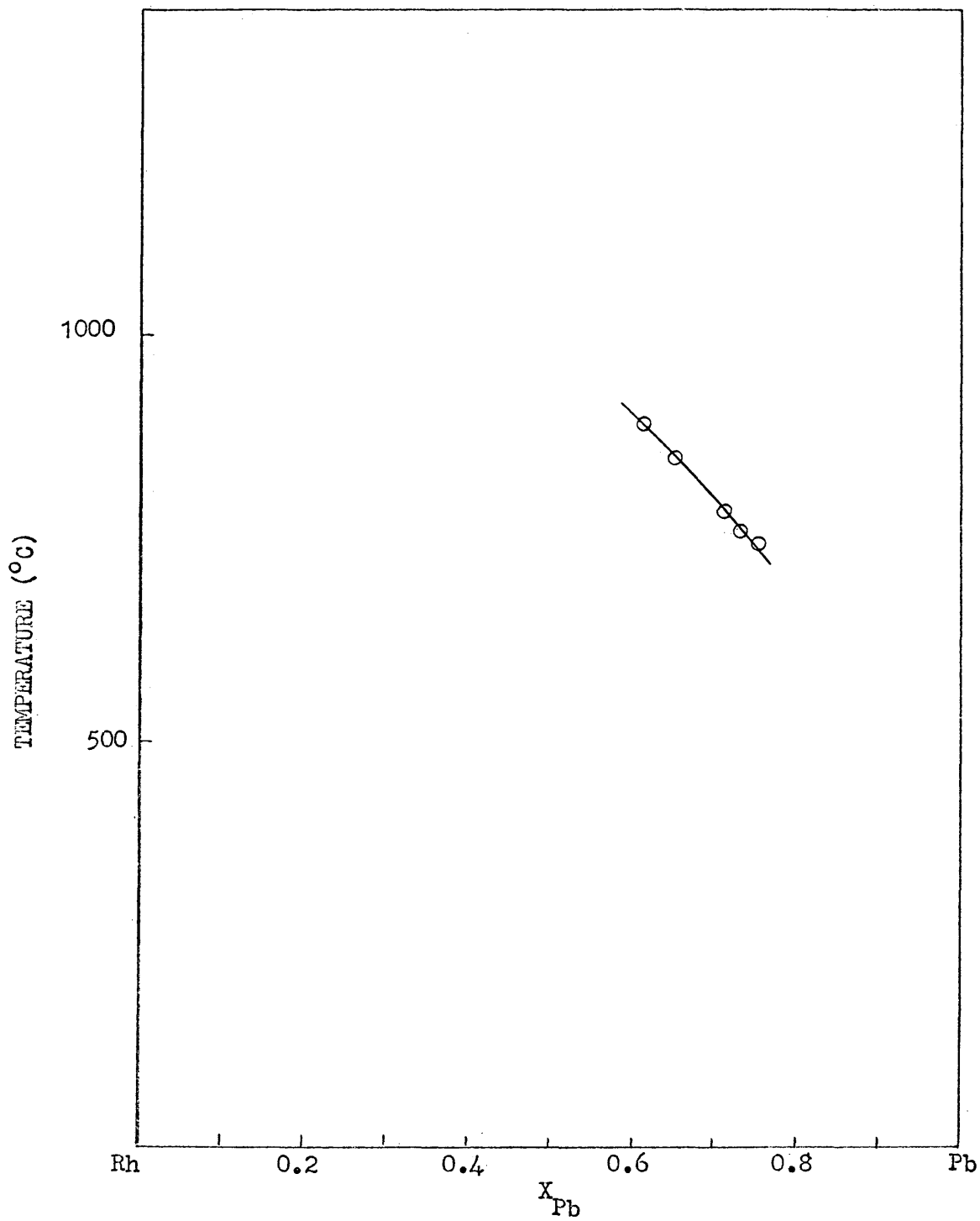


Figure 12: Liquidus portion of the lead-rhodium system.

The emf is a linear function of temperature above the liquidus line since the entropy of mixing of the homogeneous liquid alloys is independent of temperature. When a heterogeneous alloy of liquid + solid is present, there is a break in the E vs T curve. In a heterogeneous region at a given temperature, all the liquids have the same composition; therefore, they have the same potential. Hence, the E vs T plots of alloys of different overall composition should fall on a single line below the liquidus break. Each intersection of the linear portion with the liquidus on the E vs T plot yields the liquidus temperature for an alloy of that composition.

Comparison with Models of Metallic Solutions

There are three solution models which can be used to predict the thermodynamic behavior of certain liquid alloy systems. These models are the ideal, regular, and sub-regular solutions.

An ideal solution is one where

$$(1) H^M = 0$$

$$(2) S^M = S^M_{(\text{ideal})}$$

$$(3) V^M = 0$$

$$(4) \alpha_i = 0, \text{ therefore } a_i = X_i.$$

A regular solution is one where

- (1) $H^M \neq 0$
- (2) $S^M = S^M_{(\text{ideal})}$
- (3) $\alpha_i = \text{constant}$

A subregular solution is one where.

- (1) $H^M \neq 0$
- (2) $S^M = S^M_{(\text{ideal})}$
- (3) α_i is a linear function of composition.

The lead-rhodium system does not seem to fit any of these models.

CONCLUSIONS

The present study of the thermodynamic properties of liquid Pb-Rh alloys leads to the following conclusions:

1. The galvanic cell technique using a PbO-SiO_2 electrolyte is adequate for studying the thermodynamic properties of Pb-Rh alloys in the temperature range of 725°C to 1000°C .
2. A long period of time is needed to insure the alloy-electrolyte equilibration.
3. The errors due to the displacement and dissociation reactions are negligible.
4. The activity of lead shows a negative deviation from Raoult's Law.
5. A portion of the phase diagram was constructed for this study.
6. The lead-rhodium system does not agree with any of the current solution models.

SUGGESTIONS FOR FURTHER WORK

The phase diagram for the lead-rhodium system has not been determined. An attempt was made to locate some points for the phase diagram. More alloys should be studied to throw some light on the phase diagram. It would be difficult to study the alloys all the way down to $X_{Pb} = 0$. The PbO-SiO₂ electrolyte is not stable above 1030°C; hence it would not be feasible to study alloys where $X_{Pb} < 0.5$.

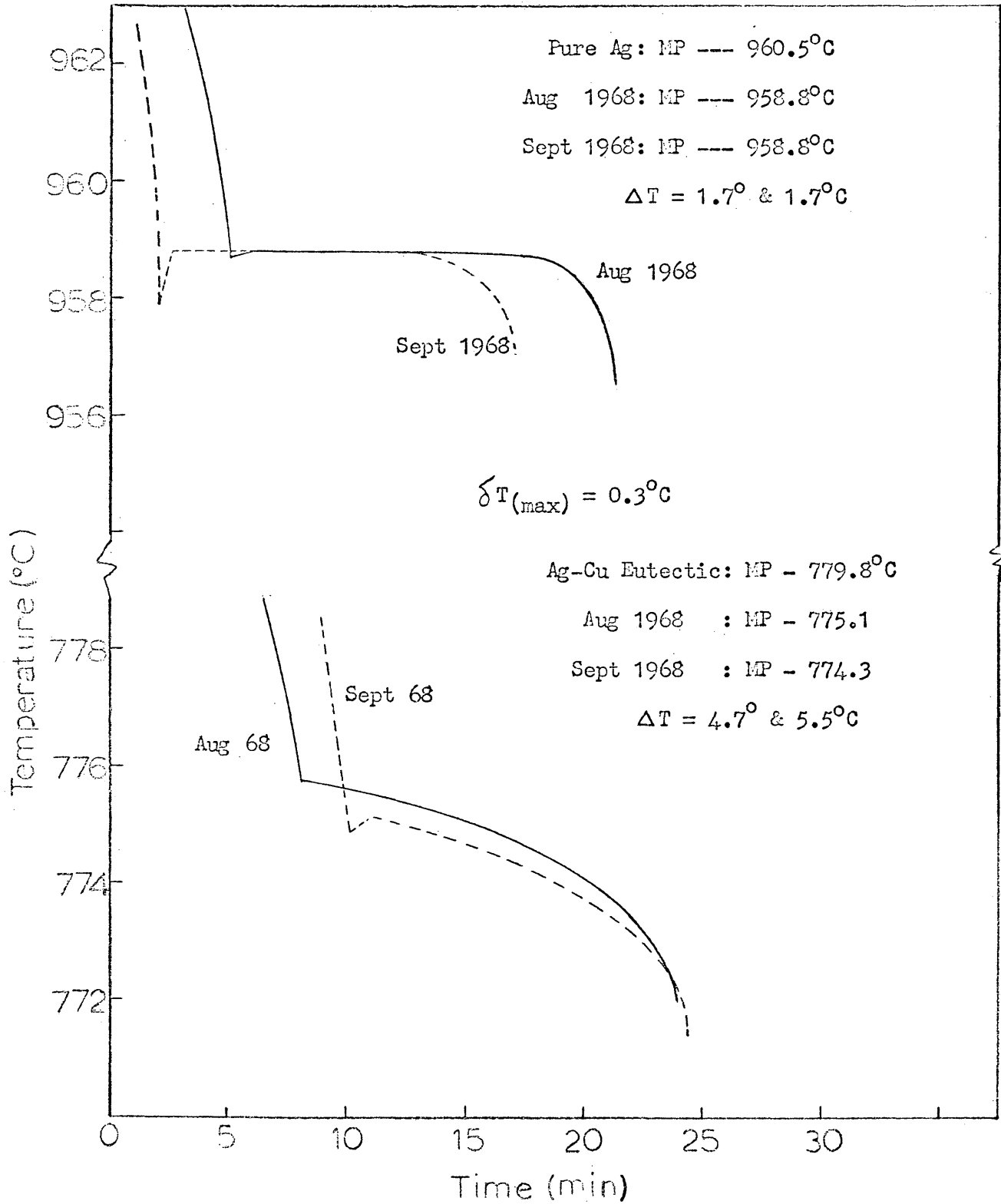
The same electrolyte could be used to study other platinum group metals alloyed with lead. The cell would be of the same type as that shown in equation (11) with one of the platinum group metals replacing rhodium.

The same electrolyte could also be used in determining interaction parameters in systems which have already been studied. Lupis and Elliott⁽²⁰⁾ have summarized the interaction parameters. Boorstein and Behlke⁽²¹⁾ have determined the interaction parameter for cadmium on tin in liquid bismuth by the use of a galvanic cell. A general technique has been outlined⁽²²⁾, following the workers just mentioned, to study the interaction between lead and gold in liquid silver. The experimental setup would be exactly similar to the one used in this study. The same electrolyte could also

be used.

A new electrolyte could be developed to study systems besides those containing lead. Wollenweber⁽¹⁸⁾ and Arismendi⁽¹⁹⁾ have done some preliminary work on $\text{Li}_2\text{O-MgO-SiO}_2$. An oxide of the less noble metal could be added in a small quantity to the above electrolyte, and systems involving a different metal could be studied. However more work has to be done on the electrolyte first.

APPENDIX II: Calibration of Thermocouple



APPENDIX III: Chemical Analyses of Materials.

1. Spectrographic Analysis of Lead

Sb	N.D.
Tl	N.D.
Mg	2
Mn	N.D.
Pb	99.99+%
Sn	N.D.
Si	N.D.
Cr	N.D.
Fe	1
Ni	N.D.
Bi	1
Al	N.D.
Ca	N.D.
Ag	N.D.
Cu	3
In	N.D.
Cd	N.D.
Zn	N.D.
Au	N.D.

N.D. = None Detected

Impurities in ppm

APPENDIX III: (Continued)

2. Chemical Analysis of the Lead Oxide

	<u>J. T. Baker</u>	<u>Mallincrodt</u>
Assay (PbO)	99.0%	---
Insoluble in CH ₃ COOH	0.010%	0.15%
Chloride (Cl)	0.001%	0.005%
Nitrate (NO ₃)	0.010%	0.01%
Silver (Ag)	0.0001%	0.0001%
Copper (Cu)	0.003%	0.002%
Iron (Fe)	0.0005%	0.005%
Substances not ppt by H ₂ S	0.02%	0.20%
Loss on ignition	---	0.5%

The SiO₂ used was 50/200 mesh silica for chromatographic columns. G. Frederick Smith Chemical Co.

BIBLIOGRAPHY

1. Taylor, N. W., The activity of Zn, Cd, Sb, Pb, and Bi in their ternary liquid mixtures: Jour. Am. Chem. Soc., v. 45, p. 2895 (1923).
2. Wagner, C., and Werner, A., The role of displacement reactions in the determination of activities in alloys with the aid of galvanic cells: Jour. of Electrochem. Soc., v. 114, no. 4, p. 326-332 (1963).
3. Hager, J. P., and Wilkomirsky, I. A., Thermodynamic properties of the lead-silver system: Trans. AIME, v. 242, p. 183-189 (1969).
4. Hager, J. P., and Walker, R. A., Emf measurements on the liquid lead-gold system using a molten oxide electrolyte: Trans. AIME, Submitted for publication.
5. Krakau, K. A., and Vakhramer, N. A., Equilibrium diagram of PbO-SiO₂ system: Keram I Steklo, v. 8, p. 42 (1932).
6. Geller, R. F., Creamer, A. S., and Bunting, E. N., The PbO-SiO₂ system: Jour. Research Natl. Bur. Standards, v. 13, p. 237 (1934).
7. Callow, R. T., The activity of PbO in the PbO-SiO₂ melts: Trans. Faraday Soc., v. 47, p. 370 (1951).
8. Preston, E., and Turner, W. E. S., The vapor pressure of PbO in PbO-SiO₂ melts: Jour. Soc. Glass Technology, v. 14, p. 296 (1935).
9. Richardson, F. D., and Webb, L. E., Oxygen in molten lead and the thermodynamics of lead-oxide-silica melts: Trans. Inst. Mining and Metall., v. 64, p. 529-564 (1955).
10. Ito, H., and Yanagase, T., Studies on lead silicate melts: Trans. Japan Inst. Metals, v. 56, p. 2931 (1962).

11. Shartis, L., and Newman, E. S., Energy relation in PbO-SiO₂ melts: Jour. Research Natl. Bur. Standards, v. 40, p. 471 (1948).
12. Sridhar, R., and Jeffre, J. H. E., Thermodynamics of PbO-SiO₂ melts: Inst. of Mining and Metall., v. 238, p. 44-50 (1967).
13. Bockris, T. O'M., Kitchener, J. A., and Davies, A. E., Electric transport in liquid silicates: Trans. Faraday Soc., v. 54, p. 536-548 (1952).
14. Bockris, T. O'M., and Mellors, G. W., Electric conductance in liquid lead silicates and borates: Jour. Phys. Chem., v. 60, p. 1321-1328 (1956).
15. Hansen, M., Constitution of binary alloys: New York, 2nd ed., p. 1096-1098 (1958).
16. Zambrano, A. R., Emf measurements on the liquid lead-silver-gold system using a molten oxide electrolyte: Golden, Colorado, Colorado School of Mines, T-1176, 94 p. (1968).
17. Topping, J., Errors of observation and their treatment: London, 3rd ed., Chapman and Hall Ltd., p. 16-24 (1966).
18. Wollenweber, C., A high temperature galvanic cell study using a PbO-SiO₂ electrolyte: Golden, Colorado, Colorado School of Mines, T-1208, 80 p. (1968).
19. Arismendi, J., High temperature thermodynamic properties of Pb-Pt alloys: Golden, Colorado, Colorado School of Mines, T-1209, 77 p. (1968).
20. Lupis, C. H. P., and Elliott, J. F., Generalized interaction coefficients: Acta Metallurgica, v. 14, p. 529-538 (1966).
21. Boorstein, W. M., and Pehlke, R. D., Galvanic cell measurement of the thermodynamic interaction between cadmium and tin in liquid bismuth: Jour. Electrochem. Soc., v. 111, no. 11, p. 1269-1272 (1964).
22. Mehta, M., Proposal for a galvanic cell study of the thermodynamic interaction between lead and gold in liquid silver: Golden, Colorado, Colorado School of Mines, unpublished (1968).

BIOGRAPHICAL NOTE

The author was born in Calcutta, India, on January 14, 1944. He received his entire pre-college education at the Calcutta Boys' School. In July 1962 he entered the Colorado School of Mines, and received his professional degree in metallurgy in June 1966. He returned to Mines in September 1967 to obtain his Master of Science degree.